

First-principles study of the atomic-scale structure of clean silicon tips in dynamic force microscopy

V. Caciuc

Physikalisches Institut, Westfälische Wilhelms Universität Münster, Wilhelm-Klemm-Str. 10, D-48149 Münster, Germany

H. Hölscher

*Center for NanoTechnology (CeNTech), Gievenbecker Weg 11, D-48149 Münster, Germany
and Physikalisches Institut, Westfälische Wilhelms Universität Münster, Wilhelm-Klemm-Str. 10, D-48149 Münster, Germany*

S. Blügel

Institut für Festkörperforschung, Forschungszentrum Jülich, D-52425 Jülich, Germany

H. Fuchs

*Center for NanoTechnology (CeNTech), Gievenbecker Weg 11, D-48149 Münster, Germany
and Physikalisches Institut, Westfälische Wilhelms Universität Münster, Wilhelm-Klemm-Str. 10, D-48149 Münster, Germany*

(Received 10 February 2006; revised manuscript received 16 March 2006; published 17 October 2006)

In the present work we report on our *ab initio* pseudopotential calculations based on density functional theory to investigate the atomic-scale behavior of clean silicon tips in noncontact atomic force microscopy (AFM). The AFM tip structures are modeled by silicon clusters with [111] and [001] termination. The structural changes induced by their reciprocal interaction are investigated by calculating the short-range chemical forces during a vertical approach and retraction of one silicon tip on top of another tip. For a specific tip geometry with [111] termination, the theoretical force curves exhibit an hysteretic behavior only at the first approach and retraction cycle. The absence of this effect at the second scan is due to sharpening of the initially blunt tip via short-range chemical forces. A specific finger print of the [001]-oriented tip is an energy dissipation induced by a breaking and formation process of a chemical bond between two silicon atoms under its apex atom.

DOI: [10.1103/PhysRevB.74.165318](https://doi.org/10.1103/PhysRevB.74.165318)

PACS number(s): 68.37.Ps, 71.15.Dx

I. INTRODUCTION

The atomic force microscope¹ (AFM) has been developed as a tool for real-space imaging of conductor, semiconductor and insulator surfaces. True atomic resolution on these surfaces (i.e., the ability of resolving pointlike defects) is currently obtained in the noncontact (NC) atomic force microscopy (AFM).^{2,3} Recent developments of this technique and its exciting applications in surface science are summarized in Refs. 4–7.

The NC-AFM relies on the measurement of the forces acting between an atomically sharp tip and a sample surface. For semiconductor^{8–10} and insulator^{11–13} surfaces, the mechanism of the atomic-scale contrast is by now well established. It was shown in these theoretical studies that for a semiconductor surface the atomic resolution is due to the short-range chemical tip-surface interactions while for an insulator surface it originates from the short-range electrostatic tip-sample forces. Recent progress has been done in understanding the origin of the image contrast mechanism on metallic surfaces.^{14,15}

From experimental point of view, a stable operating regime in NC-AFM which provides reproducible atomic-scale images is quite often difficult to be reached. The basic reason of this difficulty lies in a nonmonotonic variation of the tip-surface interaction as a function of the tip-sample separation distance. This implies a nonmonotonic imaging signal in NC-AFM while a stable NC-AFM operating regime requires

a monotonic branch in the tip-sample force curves to ensure a stable feedback.^{16–18}

Another reason lies in the fact that the geometrical and chemical structure of the AFM tip apex during the imaging process may change. This scenario is strongly supported by experimental observation that atomic-scale resolution of the sample appears or disappears after a “crash” of the tip into the sample surface.¹⁹

Consequently, it is of great interest to get an insight into the role of the geometry and structural changes of the AFM tip on the NC-AFM imaging process. To some extent, such *ab initio* studies have been performed in the past for semiconductor^{15,20,21} and insulator^{22,23} surfaces. However, due to the computational time restrictions, these studies were confined to a particular choice of the AFM tip with a specific apex geometry and chemical nature of the front atoms. Moreover, the details of the tip’s behavior might be particular to the specific surface under investigation. As previously mentioned, a key point in NC-AFM is represented by the fact that the precise atomic structure of the tips used in experiments is not known. This common situation represents a formidable challenge for theory since there is no *a priori* clear hint how to model the AFM tip in a specific experiment. A possible choice is to consider a clean silicon tip which also might become contaminated with surface atomic species during the NC-AFM scanning process on a semiconductor^{8,20,21} or metallic¹⁵ surface. For an ionic surface, the AFM tip was sometimes modeled by a MgO cluster^{12,13,24,25} accounting for

oxidized silicon tips. The effect of the silicon tip's contamination with water from vacuum chamber on the recorded NC-AFM images has also been investigated.^{15,23}

In a recent paper²⁶ we reported on our first-principle simulations aimed to investigate the possible structural changes of clean silicon tips during the NC-AFM imaging process and their implications on the contrast of the recorded images. To reach this aim, we have investigated those structural changes induced by the *tip-tip* interactions. The basic motivation of this choice is that we would like to unveil those features which describe an intrinsic behavior of clean silicon tips in some external potential which might originate from one or another surface. Nevertheless, it is important to note that such a tip-tip system is not artificial in the sense that NC-AFM experiments can be performed in principle on such systems (even if the practical difficulties are not at all negligible).

In this article we present an extended and more detailed analysis of the interaction between silicon tips with [111] and [001] terminations. For [111]-oriented silicon tips we considered clusters of different sizes and apex structures. For a certain apex configuration of such a tip, our *ab initio* simulations revealed an intrinsic sharpening process of its geometrical structure via short-range chemical forces. In this case, the theoretical force curves describing its interaction with other tips exhibit a hysteresis only during the first vertical approach and retraction path while this behavior is absent during the second oscillation cycle. The [001]-oriented silicon tip reveals a specific hysteric behavior associated with the breaking and formation of a chemical bond between two of its front atoms.

II. TIP MODEL AND COMPUTATIONAL METHOD

As largely described in literature (see, for instance, Refs. 7 and 20), the macroscopic AFM tip is modeled in simulations by a nanotip attached to a macroscopic body. The nanotip is employed in *ab initio* or semiempirical calculations in order to evaluate the short-range chemical (electrostatic) interactions responsible for the atomic-scale contrast in NC-AFM. The macroscopic part of the tip is usually used to calculate the contribution of the long-range forces on the frequency shift.²⁷ Typically, the macroscopic tip is modeled by a sphere or cone-sphere geometry whose geometrical parameters are adjusted such that the calculated frequency shift matches the experimental one. Since this contribution is lattice site independent and does not lead to atomic-scale contrast in NC-AFM, in the following we will focus only on the nanotips.

In our first-principles simulations we modeled the nano tips by clusters of silicon atoms cut along [111] and [001] directions of the bulk silicon. For silicon tips with [111] termination we considered atomic clusters of different sizes. Figure 1(a) shows the $\text{Si}_{13}\text{H}_{15}$ cluster which was used as a prototype for a Si(111)-type tip. In order to examine possible size dependent effects of this tip we also considered a smaller cluster of this type of tip. Figure 1(e) displays the Si_7H_{12} cluster of this "small" Si(111)-type tip. Please note that, from structural point of view, the Si_7H_9 cluster repre-

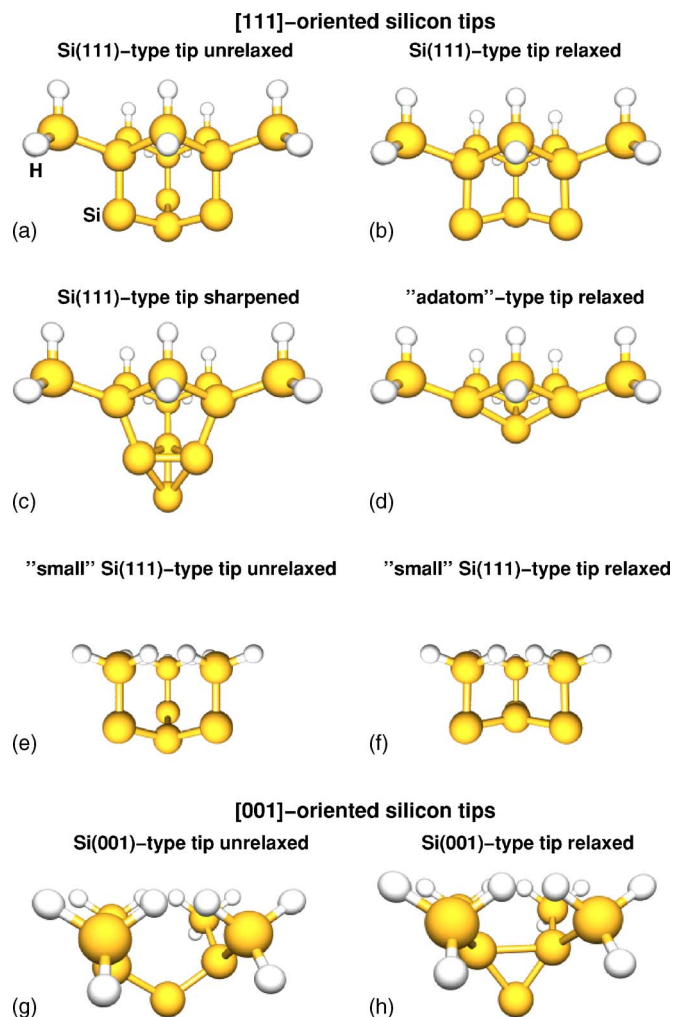


FIG. 1. (Color online) Ball-and-stick model of the atomic structure of the isolated silicon tips with [111] and [001] termination. (a) The unreaxed structure of a tip cut along [111] direction of the bulk silicon as modeled by a $\text{Si}_{13}\text{H}_{15}$ cluster [Si(111)-type tip] shows a sharp geometrical configuration with one front atom. (b) The relaxed structure of this cluster corresponds to a blunt tip with four front atoms. (c) The sharpened structure of the initially blunt Si(111)-type tip due to short-range chemical interactions. (d) By removing three front atoms of the Si(111)-type tip one obtains a tip modeled by a $\text{Si}_{10}\text{H}_{15}$ cluster (adatom-type tip). (e) The unreaxed structure of the Si_7H_9 cluster ["small" Si(111)-type tip] which represents the apex structure of the Si(111)-type tip. (f) The relaxed geometry of this tip exhibits the same blunt structure of its apex configuration in a similar fashion as for Si(111)-type tip. Note that this small cluster becomes also sharp as Si(111)-type tip when interacting with other silicon tips. (g) The unreaxed structure of an [001]-oriented tip as modeled by a Si_7H_{12} cluster [Si(001)-type tip]. (h) The relaxed structure of the Si(001)-type tip shows the formation of a chemical bond between two silicon atoms below to front atom.

sents the apex part of Si(111)-type tip and resembles the [111]-oriented tip used by Huang *et al.*²⁸ in their first-principles calculations.

Another nano tip with [111] orientation is the so-called "adatom-type" tip [Fig. 1(d), $\text{Si}_{10}\text{H}_{15}$] which was extensively

used to investigate the NC-AFM imaging mechanism on semiconductor surfaces.^{20,29–31} Furthermore, it was used for simulations on insulating surfaces in order to prove the ability of NC-AFM to chemically identify the atomic species on such surfaces.^{32,33}

As a model for a tip with [001] termination we used a Si_7H_{12} cluster [Si(001)-type tip; Fig. 1(g)]. A similar but smaller cluster was assumed before by Huang *et al.*²⁸ in order to simulate the tip-sample interaction of a Si(001)-type tip with the Si(111)- 7×7 surface.

The change of the geometrical structure of the nano tips due to their reciprocal interaction was considered by fixing the silicon atoms of their base (6 atoms for $\text{Si}_{13}\text{H}_{15}$ and $\text{Si}_{10}\text{H}_{15}$ clusters, four atoms for Si_7H_9 and three atoms for Si_7H_{12} ones) while all other silicon atoms were allowed to relax. The hydrogen atoms have been used only to saturate the base of the silicon tips and they were also kept fixed during atomic relaxations.

Our choice for pure (uncontaminated) silicon tips relies on the assumption that, with a careful preparation in ultra-high vacuum by heating and sputtering with noble-gas atoms, clean tips can be obtained and subsequently used in experiments. Of course, during an NC-AFM experiment an initially clean tip may become contaminated by crashing into the surface or picking up atoms from it.¹⁹ However, the details of such a scenario are specific to the surface under study and even for a certain surface it is almost impossible to foresee which surface's atoms are likely to attach to an AFM tip if such a process indeed takes place.

The geometry of the isolated and interacting silicon tips mentioned above has been analyzed by carrying out first-principles simulations based on density functional theory³⁴ in the local density approximation.³⁵ The total energy calculations have been performed using the pseudopotential method³⁶ as implemented in the ESPRESSO package.³⁷ In the case of silicon atoms the electron-ion interactions are described by a von Barth and Car³⁸ norm-conserving pseudopotential⁴³ while the bare Coulomb potential was used for hydrogen atoms. The silicon tips were placed in orthorhombic supercells of $18 \times 18 \times 20$ Å. For this setup, the Kohn-Sham orbitals were expanded over a plane wave basis set generated by a cutoff energy E_{cut} of 45.0 Ry. With this choice, the theoretical lattice parameter of bulk silicon has a value of 5.407 Å, very close to that reported in Ref. 39 (5.398 Å). The Brillouin zone integrations have been done using the Gamma point. Finally, the geometrical structure of the silicon tips was optimized with an accuracy of the calculated interaction forces better than 5×10^{-5} Ry/(atomic units).

III. SIMULATION RESULTS

A. Isolated silicon tips

From physical point of view, an isolated silicon tip describes the case when the tip mounted at the free end of the cantilever is far away from the sample surface. This occurs, for instance, in the early stage of preparing the AFM microscope to scan a surface in which the tips are sputtered with

noble-gas ions and heated to clean them from atomic impurities.

For silicon tips with [111] termination one obvious choice is to consider the atomic cluster depicted in Fig. 1(a). To investigate the role of the size of such a cluster on its relaxed configuration, a smaller cluster Si_7H_9 [see Fig. 1(e)] describing its apex part was also taken into account. A similar tip was used by Huang *et al.*²⁸ together with a [001]-terminated tip in order to establish if the atomic orbitals can be resolved by NC-AFM as suggested by Giessibl *et al.*⁴⁰

In this unrelaxed configuration, the $\text{Si}_{13}\text{H}_{15}$ cluster exhibits one dangling bond due to a bulklike threefold coordination of its apex atom. However, when relaxing the atomic positions of seven front atoms, the resulting structure presented in Fig. 1(b) shows a strong relaxation of the four apex atoms of the initial structure. This atomic relaxation process is accompanied by a total energy difference between the relaxed and unrelaxed structures of about -1.04 eV. In consequence, this tip is intrinsically blunt. This feature suggests that the use of such a tip in NC-AFM cannot provide atomic-scale resolution. This might be also the reason why so far it was never used in simulations to model a nanotip. The Si_7H_9 tip exhibits the same behavior when relaxing its four front atoms as shown in Fig. 1(f). Therefore, we conclude that a blunt apex structure of the Si(111)-type tip is not caused by a size dependent effect.

Another option for a [111]-oriented silicon tip is to consider a $\text{Si}_{10}\text{H}_{15}$ cluster [see Fig. 1(d)]. This tip is structurally related to the Si(111)-type one. More specifically, by removing three from four apex atoms of the $\text{Si}_{10}\text{H}_{15}$ cluster, the remaining front atom is captured by the rest of the cluster leading to this “adatom-type” silicon tip. The geometrical and electronic structure of this type of tip are extensively discussed in the literature (see, for example, Ref. 9, and references therein). It was shown in these studies that this tip has one dangling bond containing one electron. Furthermore, from mechanical point of view, this tip is a stiff one and only its apex atom exhibits a significant relaxation during the interaction with a surface.

The unrelaxed structure of a silicon tip with [001] termination is presented in Fig. 1(g). Starting from this unrelaxed configuration and allowing the three front atoms to move according to the calculated Hellmann-Feynman forces, the relaxed structure of the Si_7H_{12} tip was obtained and shown in Fig. 1(h). The basic difference between the relaxed and unrelaxed structures consists in the formation of a chemical bond between two silicon atoms underneath the front atom. This behavior originates from the fact that both silicon atoms already had one dangling bond. It is interesting to note that, as already reported in Ref. 26, the calculated charge density of this type of tip did not exhibit a “two-dangling bond” feature as was sometimes assumed in literature [see Fig. 2(c) in Ref. 26]. It is important to note that this is also true when this type of tip interacts with other silicon tips (see below).

B. The tip-tip interactions

As already mentioned in the Introduction, the basic aim of the present study is to investigate possible structural changes

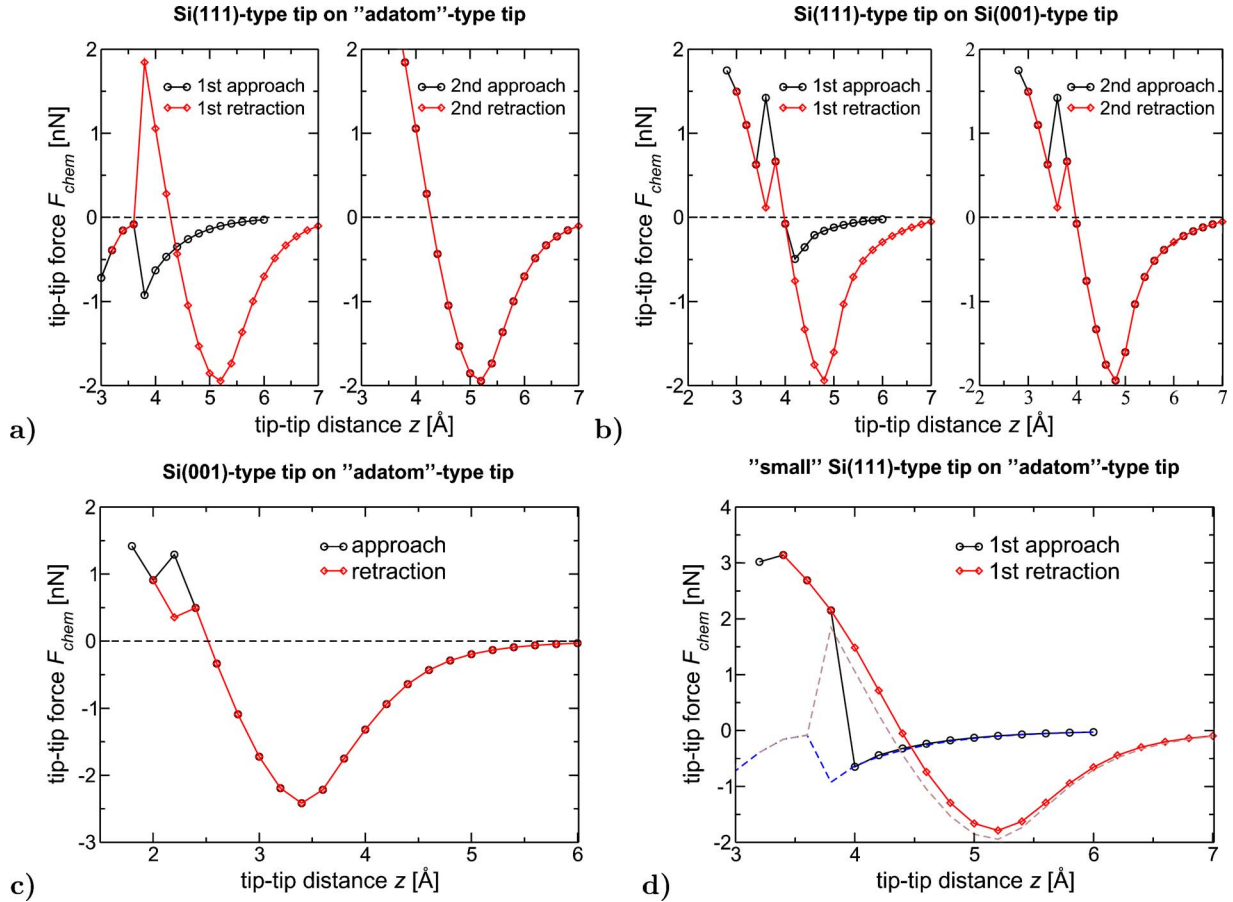


FIG. 2. (Color online) The normal component of the short-range tip-tip chemical force F_{chem} due to the interaction between silicon tips with [111] and [001] termination. (a) The force curves corresponding to the interaction between the Si(111)-type tip [Fig. 1(b)] and the adatom-type one [Fig. 1(d)] show a large hysteresis during the first approach and retraction cycle. However, there is no hysteresis during the second scan. The origin of this behavior lies in an irreversible structural change of the Si(111)-type tip such that this tip becomes sharp and stable (the corresponding structural changes are presented in Fig. 3). (b) The same qualitative behavior is displayed by the interaction between the Si(111)-type tip [Fig. 1(b)] and Si(001)-type [Fig. 1(h)] one. As in the previous case, the absence of the hysteresis during the second approach and retraction path is associated with the sharpening of the Si(111)-type tip. The small hysteric feature when the tips are 3.4 Å apart is due to the breaking (formation) of a chemical bond between two silicon atoms of the Si(001)-type tip (see Fig. 4). (c) The small hysteresis revealed by the interaction between the Si(001)-type tip and the adatom-type one has the same origin as that discussed for Si(111)-type and Si(001)-type tips. This result also shows that, as already mentioned in literature, the adatom-type tip modeled by a $\text{Si}_{10}\text{H}_{15}$ cluster is rather stiff and its structure does not relax significantly during an NC-AFM scan. (d) The comparison between the interaction of the small Si(111)-type tip modeled by a Si_7H_9 cluster [Fig. 1(f)] and adatom-type tip with that between the Si(111)-type and adatom-type tips [plotted by dashed lines, see also Fig. 2(a)] shows that reliable interaction forces in the repulsive regime during the first scan can be obtained only when using a tip modeled by a $\text{Si}_{13}\text{H}_{15}$ cluster. However it is important to note that a similar sharpening process such as in the case of the Si(111)-type tip takes place also for the smaller Si_7H_9 cluster.

of clean silicon tips during the NC-AFM imaging process. To analyze such dynamics at atomic scale, in principle one has to consider the interaction between an AFM tip and a sample surface. As extensively discussed in literature, such an approach is a very powerful tool in understanding the mechanism of NC-AFM imaging process because it delivers a detailed picture of the atomic scale dynamics of both tip and surface under consideration. However, since our main goal is to investigate the dynamics of silicon tips in NC-AFM, in the following we will focus on those structural changes induced by tip-tip interactions. In its important to note that this option does not imply that the structural changes unveiled in this way are particular to this specific physical system. Indeed, each type of tip considered in our simulations can be thought

as modeling locally a surface (although special care must be paid to which property of the surface is modeled in this way). For instance, the adatom-type silicon tip has one dangling bond containing one electron and can be used to model, for instance, the interaction of an AFM tip with silicon adatoms on Si(111)-(7×7) surface as described in Ref. 23.

The short-range chemical tip-tip interaction force was calculated when the tips were approached and retracted on top of each other. The step used during the approach and retraction paths was set to 0.2 Å. At each step the geometrical structures of the tips were relaxed according to the calculated tip-tip interaction forces. In consequence, our *ab initio* simulations provide the history of the structural changes of the silicon tips during the approach and retraction paths, i.e., the

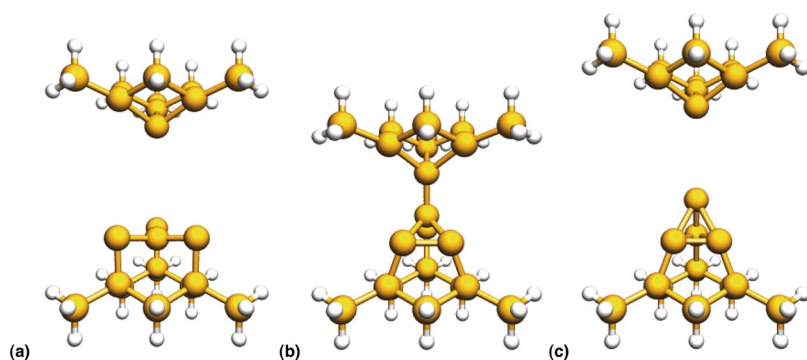


FIG. 3. (Color online) Snapshots of the atomic configuration corresponding to the interaction of two silicon tips with [111] termination. (a) Initially, the Si(111)-type (bottom) and adatom-type (up) tips are 6.0 Å apart. At this separation distance the attractive interaction between the tips is almost negligible such that their atomic structure differ very little from that of the isolated case [see Figs. 1(a) and 1(d)]. (b) During the first oscillation cycle, on the retraction path at a separation distance of 3.8 Å the initially blunt Si(111)-type tip becomes sharp due to the jump of one front atom towards the adatom-type one. (c) The sharpened Si(111)-type tip keeps its shape during the second approach and retraction cycle and thus it can provide a stable imaging process in NC-AFM. Here the tips are 7.0 Å apart on the second retraction path.

dynamics at atomic scale (from structural point of view) of the tips under consideration. As already described in Refs. 30 and 31, the tip-tip distance z used to plot the theoretical force curves corresponding to these scans is the vertical distance between the Si apex atoms of the AFM tips in their equilibrium ground state structure. The tips were approached until a multibondlike interactions occurred in the repulsive regime. This implies that starting with an average load force of 2 nN in the repulsive regime, the tips begin to “melt” into each other (in a similar way to the atomic configurations depicted in Figs. 4, 5, and 6 from Ref. 41) which would lead to a severe damage of these tips during surface’s scanning in a NC-AFM experiment.

In Fig. 2(a) we report the force curves as a function of the tip-tip distance z calculated for two silicon tips with [111] termination, modeled by a $\text{Si}_{13}\text{H}_{15}$ and $\text{Si}_{10}\text{H}_{15}$ cluster. The basic feature displayed by these theoretical force curves is the presence of a large hysteresis when the tips are approached and retracted for the first time, while this hysteretic behavior is absent at the second vertical scan. As shown in Fig. 3(b), at atomic level this remarkable feature is due to the sharpening of the Si(111)-type tip. This process takes place when the tips are 3.8 Å apart on the retraction path and is related to the jump of one front atom of the Si(111)-type tip towards the apex atom of adatom-type tip. This jump of one silicon atom leads to the formation of a tetragonally coordinated cage of silicon atoms which is, from structural point of view, much more stable than the initial configuration [see Fig. 1(c)]. From energetical point of view this implies that the total energy difference between the isolated sharpened tip and the blunt one is about -0.86 eV. In addition, when this tetragonal unit of the Si(111)-type tip is formed, the corresponding sudden shrinkage of the distance between the tips results in a strong repulsive interaction.

It is worth to note that the hysteresis present during the first scan of these tips underlies on an irreversible structural change of the blunt tip. This is at variance with the hysteric behavior of a tip-surface system, which so far was associated with a discontinuous and reversible structural changes of the tip-surface system required by a stable NC-AFM operational mode (see, for example, Chaps. 15, 16, 19 and 20 from Ref. 4). Nevertheless, as shown by our *ab initio* simulations, the

use of a blunt (soft) silicon tip leads to an additional contribution of the dissipated energy, at least in the initial stage of the imaging process. Since the adatom-type tip exhibits one dangling bond, it is very likely that the sharpening mechanism of AFM tips with similar structure via short-range chemical forces can occur on surfaces with atoms presenting similar dangling bonds.

This conclusion is further supported by a similar qualitative behavior obtained for the interaction between the Si(111)-type and Si(001)-type tips. As clearly depicted in Fig. 2(b), the first vertical scan is accompanied by a large hysteresis while the second scan exhibits only a small hysteresis in the repulsive regime when the vertical distance between the tips is 3.4 Å. Similarly to the previous case, this hysteric behavior is also due to irreversible structural changes related to the sharpening of the initially blunt Si(111)-type tip (see Fig. 4). However, when interacting with an [001]-oriented tip, the sharpening process of the blunt Si(111)-type tip occurs on the approach path while when interacting with an [111]-oriented tip this process took place on the retraction path.

Interestingly, the force curves calculated for these silicon tips with different crystallographic orientations presents a peculiar feature at the first and second vertical scan. When the tips are approached, for a tip-tip separation distance of 3.4 Å the chemical bond between the two silicon atoms underneath the front atom of Si(001)-type tip is broken. In quantitative terms, the distance which separates these atoms increases from 2.6 to 3.6 Å. On the contrary on the retraction path such a chemical bond is formed at the same tip-tip distance.

As already shown in several *ab initio* simulations performed for semiconductor surfaces,^{20,21,29,30} the $\text{Si}_{10}\text{H}_{15}$ cluster models a silicon tip cut along [111] direction which exhibits a large stiffness. The theoretical force curves corresponding to the interaction of this tip with a Si(001)-type one is shown in Fig. 2(c). For the later tip we observe the same breaking (formation) of the chemical bond between two apex atoms on the approach (retraction) path for a tip-tip distance of 2.2 Å. Therefore, one might conclude that this behavior is a specific feature of this type of tip. Except for this effect, the interaction of these tips does not show any hysteresis.

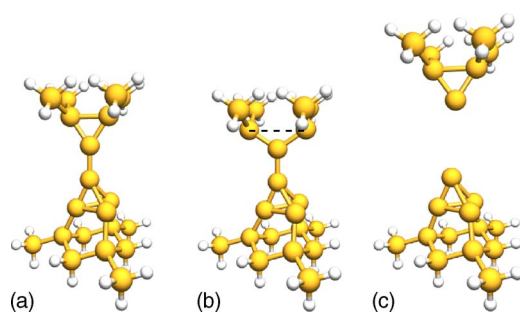


FIG. 4. (Color online) Snapshots of the atomic configuration corresponding to the interaction of silicon tips with $[111]$ and $[001]$ termination. (a) The interaction between the blunt $\text{Si}(111)$ -type tip with a $\text{Si}(001)$ -type one leads also to the sharpening of the $[111]$ -oriented tip. In this case, the sharpening process of the blunt tip takes place on the approach path of the first scan at a separation distance of 4.0 \AA . (b) The small hysteresis present in the force curves describing the interaction between these tips [see Fig. 2(c)] is related to the breaking and formation of a chemical bond of two silicon atoms (those connected by a dashed line). This chemical bond breaks when the tips are approached and it forms when they are retracted at the same separation distance of 3.4 \AA . (c) As in this case of the interaction between two $[111]$ -oriented tips [see Fig. 3(c)], the sharpened $\text{Si}(111)$ -type tip due to its interaction with $\text{Si}(001)$ -type one remains stable during NC-AFM scanning process. The $\text{Si}(001)$ -type tip also preserves its form during such vertical scan can therefore provide stable imaging mode in NC-AFM (the tips are at 7.0 \AA on the second retraction path).

An interesting observation refers to the spatial range of a noncontact operational mode when using such silicon tips. It becomes apparent from Figs. 2(b) and 2(c) that the use of an initially blunt and soft tip with $[111]$ orientation requires a larger tip-tip (sample) distances of closest approach than that needed by an initially sharp and stiff tip with the same orientation as modeled by a $\text{Si}_{10}\text{H}_{15}$ cluster.

In addition to this, the electronic structure of the interacting tip-tip systems as revealed by charge density plots of the ground-state (valence) charge density deserves some remarks. In particular, the charge density maps calculated for the $\text{Si}(001)$ -type tip when interacting with other silicon tips does not show the formation of any configuration which would exhibit two-dangling bonds. This feature is depicted in Fig. 5(a) for the case of the $\text{Si}(001)$ -type tip on top of $\text{Si}(111)$ -type one. For comparison, the charge density of two interacting (111) -type silicon tips is also shown in Fig. 5(b). One can also observe that the charge density of the $\text{Si}(111)$ -type tip looks very similar in both cases. This observation is another strong indication that the sharpening process of this tip is an intrinsic effect of the $\text{Si}(111)$ -type tip itself which is very likely to take place when the tip approaches a surface.

Finally, an important observation concerns the size of the tips used in our first-principles simulations and the number of atoms to be relaxed when modeling silicon tips. As depicted in Fig. 2(d), our calculations performed with a smaller blunt Si_7H_9 cluster by relaxing only its first four front atoms showed that its interaction with an adatom-type tip agrees nicely up to a distance of 4.0 \AA with the results obtained

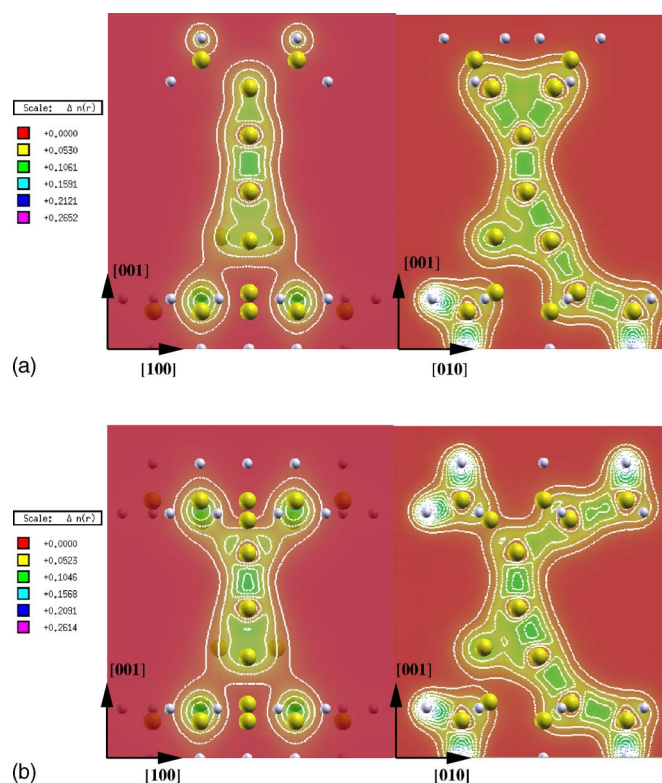


FIG. 5. (Color online) (a) Charge density plots corresponding to the interaction of the $\text{Si}(111)$ -type tip with the $\text{Si}(001)$ -type one in the configuration sketched in Fig. 4(a). Similarly to the isolated (001) -type tip [see Fig. 2(c) in Ref. 26], the charge density of this tip exhibits also an axial symmetry and does not show any “two-dangling bond” feature. Please, note the strong chemical interaction between the apex atoms of both type of tips. (b) The charge density plots corresponding to the interaction between a $\text{Si}(111)$ -type tip and the adatom-type one for the geometry drawn in Fig. 3(b). The charge accumulation in the region separating the apex atoms of these tips indicate as in the previous case a strong chemical interaction between these tips which leads to the sharpening of the $\text{Si}(111)$ -type tip. The maps of the ground-state charge density have been obtained using the XCRYSDEN program (Ref. 42).

when using a larger $\text{Si}_{13}\text{H}_{15}$ cluster. However, for tip-tip separation distances smaller than 4.0 \AA the tip-tip interaction becomes repulsive when using the “small” $\text{Si}(111)$ -type tip while it is still attractive in the case of the larger tip. Also the magnitude of repulsive forces is larger in the case of using a smaller tip than a larger one. However, on the retraction path, at separation distances larger than 5.0 \AA the force curves calculated for both cases are quite comparable.

It is interesting to note that, despite of its rather small size, the interaction of the Si_7H_9 cluster with the adatom-type tip leads also to the sharpening of this cluster in a similar way as already mentioned for the $\text{Si}(111)$ -type tip. This observation enable us to conclude that this sharpening process of $\text{Si}(111)$ -type tip is a general feature of this type of tip. In addition to this, for the sharp adatom-type tip only the apex atom relaxes significantly, the relaxation of the next three atoms in the layer underneath being rather small.

IV. SUMMARY

By using the *ab initio* pseudopotential method, we have investigated the atomic-scale dynamics of silicon tips with [111] and [001] termination as revealed by their reciprocal interaction. For a (111)-type tip, we considered atomic clusters with different geometrical structure. For one specific structure modeled by a $\text{Si}_{13}\text{H}_{15}$ cluster, our first-principles simulations evidenced a possible mechanism for sharpening of an initially blunt tip via short-range chemical forces. This sharpening process is associated with an irreversible structural change of this tip and leads to an additional dissipation channel in NC-AFM in the early stage of the imaging process. Since this behavior is common to the interaction of this tip with an adatom-type tip which has one dangling bond as well as with a tip cut along [001] direction, we expect that such a mechanism is possible also on surfaces. After this process

has taken place, a stable NC-AFM imaging mode becomes possible.

For the silicon tip with [001] termination, our simulations reveal a peculiar structural change of this type of tip. This structural change is associated with a specific hysteresis pattern which is based on a chemical bond breaking (formation) between two of its front atoms on the approach and retraction path.

ACKNOWLEDGMENTS

The computations were performed with the help of the ZIVCLUSTER at the WWU Münster and the Forschungszentrum Jülich (Grant "Rasterkraftmikroskopie"). This work was financially supported by the DFG (Grant No. HO 2237/2-1) and the BMBF (Grant No. 03N8704).

- ¹G. Binnig, C. F. Quate, and C. Gerber, *Phys. Rev. Lett.* **56**, 930 (1986).
- ²F. J. Giessibl, *Science* **267**, 68 (1995).
- ³Y. Sugawara, M. Otha, H. Ueyama, and S. Morita, *Science* **270**, 1646 (1995).
- ⁴S. Morita, R. Wiesendanger, and E. Meyer, *Noncontact Atomic Force Microscopy* (Springer, Berlin, 2002).
- ⁵R. García and R. Pérez, *Surf. Sci. Rep.* **47**, 197 (2002).
- ⁶F. J. Giessibl, *Rev. Mod. Phys.* **75**, 949 (2003).
- ⁷W. A. Hofer, A. S. Foster, and A. L. Shluger, *Rev. Mod. Phys.* **75**, 1287 (2003).
- ⁸R. Pérez, M. C. Payne, I. Štich, and K. Terakura, *Phys. Rev. Lett.* **78**, 678 (1997).
- ⁹R. Pérez, I. Štich, M. C. Payne, and K. Terakura, *Appl. Surf. Sci.* **140**, 320 (1999).
- ¹⁰I. Štich, J. Tóbiš, R. Pérez, K. Terakura, and S. H. Ke, *Prog. Surf. Sci.* **64**, 179 (2000).
- ¹¹A. I. Livshits, A. L. Shluger, and A. L. Rohl, *Appl. Surf. Sci.* **140**, 327 (1999).
- ¹²R. Bennewitz, A. S. Foster, L. N. Kantorovich, M. Bammerlin, C. Loppacher, S. Schär, M. Guggisberg, E. Meyer, and A. L. Shluger, *Phys. Rev. B* **62**, 2074 (2000).
- ¹³A. S. Foster, C. Barth, A. L. Shluger, and M. Reichling, *Phys. Rev. Lett.* **86**, 2373 (2001).
- ¹⁴I. Štich, P. Dieška, and R. Pérez, *Appl. Surf. Sci.* **188**, 325 (2002).
- ¹⁵P. Dieška, I. Štich, and R. Pérez, *Phys. Rev. Lett.* **91**, 216401 (2003).
- ¹⁶H. Ueyama, Y. Sugawara, and S. Morita, *Appl. Phys. A: Mater. Sci. Process.* **66**, S295 (1998).
- ¹⁷U. D. Schwarz, H. Hölscher, and R. Wiesendanger, *Phys. Rev. B* **62**, 13089 (2000).
- ¹⁸M. Heyde, M. Sterrer, H.-P. Rust, and H.-J. Freund, *Appl. Phys. Lett.* **87**, 083104 (2005).
- ¹⁹R. Hoffmann, L. N. Kantorovich, A. Baratoff, H. J. Hug, and H.-J. Güntherodt, *Phys. Rev. Lett.* **92**, 146103 (2004).
- ²⁰R. Pérez, I. Štich, M. C. Payne, and K. Terakura, *Phys. Rev. B* **58**, 10835 (1998).
- ²¹J. Tóbiš, I. Štich, and K. Terakura, *Phys. Rev. B* **63**, 245324 (2001).
- ²²A. L. Shluger, L. N. Kantorovich, A. I. Livshits, and M. J. Gillan, *Phys. Rev. B* **56**, 15332 (1997).
- ²³A. I. Livshits, A. L. Shluger, A. L. Rohl, and A. S. Foster, *Phys. Rev. B* **59**, 2436 (1999).
- ²⁴A. L. Shluger, A. L. Rohl, R. T. Williams, and R. M. Wilson, *Phys. Rev. B* **52**, 11398 (1995).
- ²⁵A. I. Livshits and A. L. Shluger, *Phys. Rev. B* **56**, 12482 (1997).
- ²⁶V. Caciuc, H. Hölscher, S. Blügel, and H. Fuchs, *Phys. Rev. Lett.* **96**, 016101 (2006).
- ²⁷F. J. Giessibl, *Phys. Rev. B* **56**, 16010 (1997).
- ²⁸M. Huang, M. Čuma, and F. Liu, *Phys. Rev. Lett.* **90**, 256101 (2003).
- ²⁹S. H. Ke, T. Uda, R. Pérez, I. Štich, and K. Terakura, *Phys. Rev. B* **60**, 11631 (1999).
- ³⁰J. Tóbiš, I. Štich, R. Pérez, and K. Terakura, *Phys. Rev. B* **60**, 11639 (1999).
- ³¹S. H. Ke, T. Uda, I. Štich, and K. Terakura, *Phys. Rev. B* **63**, 245323 (2001).
- ³²A. S. Foster, A. Y. Gal, J. M. Airaksinen, O. H. Pakarinen, Y. J. Lee, J. D. Gale, A. L. Shluger, and R. M. Nieminen, *Phys. Rev. B* **68**, 195420 (2003).
- ³³A. S. Foster, A. Y. Gal, J. D. Gale, Y. J. Lee, R. M. Nieminen, and A. L. Shluger, *Phys. Rev. Lett.* **92**, 036101 (2004).
- ³⁴W. Kohn and L. J. Sham, *Phys. Rev.* **140**, A1133 (1965).
- ³⁵J. P. Perdew and A. Zunger, *Phys. Rev. B* **23**, 5048 (1981).
- ³⁶M. C. Payne, M. P. Teter, D. C. Allan, T. A. Arias, and J. D. Joannopoulos, *Rev. Mod. Phys.* **64**, 1045 (1992).
- ³⁷S. Baroni *et al.*, <http://www.pwscf.org/>.
- ³⁸U. von Barth and R. Car (unpublished).
- ³⁹P. Giannozzi, S. de Gironcoli, P. Pavone, and S. Baroni, *Phys. Rev. B* **43**, 7231 (1991).
- ⁴⁰F. J. Giessibl, S. Hembacher, H. Bielefeldt, and J. Mannhart, *Science* **289**, 422 (2000).
- ⁴¹M. R. Jarvis, R. Perez, and M. C. Payne, *Phys. Rev. Lett.* **86**, 1287 (2001).
- ⁴²A. Kokalj, *J. Mol. Graphics Modell.* **17**, 176 (1999).
- ⁴³The pseudopotentials used in our simulations are provided by ESPRESSO package and can be downloaded from www.pwscf.org/pseudo.htm.